Dynamic Feasibility Assessment of Ship-to-Grid Interconnection by DC-Link

Sobhan Badakhshan, *Student Member, IEEE*, Soroush Senemmar, *Student Member, IEEE*,
and Jie Zhang, *Senior Member, IEEE*
The University of Texas at Dallas
Richardson, TX 75080, USA
{Sobhan.Badakhshan, Soroush.Senemmar, jiezhang}@utdallas.edu

***Abstract*—The concept of ship-to-grid has been explored in recent years, which allows electric ships to supply a part of power demand in the terrestrial electric grid during normal operations or extreme conditions under disruptive events. While this could potentially enhance the resiliency of the power grid during extreme events, interconnected ship-to-grid may pose certain threats to the special equipment on the shipboard power system. To better evaluate the dynamic feasibility of ship-to-grid interconnection, this paper investigates the use of a DC-link for safely integrating a medium voltage AC (MVAC) ship to the grid. To evaluate the effectiveness of the DC-link for ship-to-grid connection, different disturbances are simulated in the shoreline grid, and their impacts on the shipboard power system are analyzed. The proposed strategy has been verified by a case study on a 4-zone shipboard power system and various shoreline grids with different characteristics. The dynamic simulations are conducted with the PSS@E and PSS@NETOMAC software.**

***Index Terms*—Shipboard Power System, Ship-to-Grid, DC-Link, Synchronization, AC to DC to AC**

I. Introduction

Electricity grids located near coastline areas are facing an increasing frequency of high-intensity power outages caused by natural disasters like hurricanes, in addition to other threats like physical and cyber attacks [1], [2]. In the U.S., inclement weather disasters have caused more than 70% of long-term power outages involving more than 50,000 electric consumers [3]. Several weather disasters (including hurricanes, floods, tornadoes, and storms) consequently led to financial damages with losses of over 1 billion dollars in 2016 in the U.S. [4]. Hurricane Harvey on Texas and Louisiana damages cost up to 180 billion dollars and catastrophic power interrupts lasted up to weeks in some regions in 2017 [5]. Other recent devastating hurricanes, such as Hurricane Irene on the east coast of the U.S., Hurricane Ike, Typhoon Soudelor, and Hurricane Sandy, had severe impacts on the power grid distribution systems, which led to widespread blackout [6], [7].

The impacts of extreme weathers on power grids underscore the need for enhancing the resiliency of the power system. There exist different strategies for power system restoration after a widespread power outage in severe weather events, including system automation, fast islanding detection schemes, rotational load shedding, special protection schemes, and mobile energy systems [8]. Among mobile energy systems, shipboard power generation has been recognized as a promising solution to supply critical loads after a major fault and help service restorations for improving terrestrial power system resiliency.

On the other hand, oceans cover over 70 percent of the Earth's surface and all of them are connected and form a massive maritime transportation system. This could be a potential solution to transmit an enormous amount of electricity all over the world, especially in emergency conditions by utilizing effective Navy ships. Thus, ships can provide energy to areas affected by the natural disaster, cyber and physical attacks, or any other contingencies when power outages regularly shut down work. There are some floating ship power plants that could dock in the harbor, crank up their turbines and start quickly generating power [9].

The challenge is that the terrestrial grids have different characteristics such as various voltage levels, grid frequencies, topologies, and short circuit ratios. However, from the shipboard power system point of view, interconnected ship-to-grid may pose certain threats to the special equipment on the shipboard power system, making the connection of ship-to-grid more challenging [10]. Many subsystems on the ship, such as generators, battery bank supplies, the electric motor of the propulsion system, navigation and cruise systems, and power electronic converters, are extremely sensitive and expensive facilities [11]. Special loads designated as high ramp rate loads (e.g., pulsed loads) have also been incorporated into the ship [12]. Generally, building a ship takes years to complete the entire basic design and the product engineering process, and the construction of military ships requires even longer time. These ships are not specifically designed to supply shoreline power system loads with the ship-to-grid connection capability. Thus, it is important to assess the dynamic feasibility of ship-to-grid connection, and ensure the stability, reliability, and safety of shipboard power systems under different types of terrestrial grid operations when connected.

A. Literature Review

There exist only a few studies in the literature on ship-to-grid integration. For example, Dabbaghjamanesh et al. [13] have investigated the coordination between the terrestrial power system and the shipboard power system under both post-disaster restoration and normal operations for improving the resiliency of distribution networks. Wen et al. [14] have

978-1-6654-7902-8/22/$31.00 ©2022 IEEE

explored the connection of different ferries that exchange power with the gird, based on the electricity price of the terrestrial grid and its impact on the ferries navigation route. Vicenzutti et al. [15] analyzed possible AC high voltage ship-to-grid connection configurations, ranging from low to medium voltage shipboard power systems. Ghimire et al. [16] have developed dynamic efficiency models for DC hybrid shipboard power system components, which are used to estimate the overall system efficiency using a realistic load power profile and a rule-based power system management. In addition to ship-to-grid studies, some works [17]–[19] have also explored load monitoring and fault detection for shipboard power systems, which are extremely useful for future unmanned surface vessels.

B. Research Objective

In modeling the shipboard power system, various components and systems in multiple energy domains and different dynamics or system time constants could significantly complicate the simulator development process. In many industrial applications, such as connecting offshore wind farms to the grid [20], connecting different microgrids [21], and machine drives [22], DC-link modules have become increasingly popular nowadays. The DC technology provides a secure and optimal control of a network's load flow, as well as quick power restoration in the event of a significant disturbance or even a blackout [23]. The DC connection can compensate for the fluctuations in the voltage, power, and frequency, which makes it an ideal technology for system loss reduction and stabilizing the terrestrial power grid. In particular, for ship-to-grid connection, the grid-connected driver is designed by an AC to DC converter in the ship side, and a DC to AC converter that is connected to the shoreline grid.

In this paper, to further enhance the feasibility of the conventional coherency-based dynamic modeling for interconnected ships, the DC-link is proposed to address the differences in voltage levels and frequencies among various shoreline grids, when leveraging electric ships for network restoration during extreme conditions. Power system dynamic equivalent models for ships and the DC-link are developed and simulated to study the ship-to-grid integration.

The remainder of the paper is organized as follows: Section II models a 4-zone shipboard power system. The DC-link connection for ship-to-grid is described in Section III. Section IV presents numerical results and discussion of a case study, followed by the conclusion in Section V.

II. Interconnected Shipboard Power System

The interconnection between a shipboard power system and a terrestrial grid will require automatic synchronization (connection), islanding (separation or decoupling), and dispatch controls. Figure 1 shows an overview of the three types of control systems, to be implemented with different measurements and coordinated protection schemes for ship-to-grid connection to enhance the resilience of power grids.

When connecting the ship to the terrestrial grid and supplying the shoreline loads, it is important to analyze the impacts of the connection on the shipboard power system. Due to the extremely sensitive and expensive facilities in the shipboard power system, in this paper we focus on studying the transient behavior of the interconnected ship-to-grid under disturbances in the shoreline grid.

The generators on shipboard could be broadly classified into two types: main generators and auxiliary generators. The main generators have larger generation capacity while the auxiliary generators will have a fractional generation capacity of main generators (e.g., less than 30%). The essential components of power generation units in shipboard power systems include generators, gas turbines, exciters, voltage regulators, rectifiers, as well as filtering modules based on the rectifier topology (for medium voltage DC ships). In this paper, the main generator is a dual wound single shaft gas turbine generator, with two independent sets of 3 phase windings, a gas turbine governor, and an excitation system with voltage regulators. Either port/starboard switchboards are supplied independently by a single generator. Shipboard power systems usually consist of different modules, such as the power conversion module, the integrated power node center, propulsion motors, and the energy storage module [24]. In grid-connected operations, the stability plays a key role in providing reliable power to both shoreline customers and the ship itself. As shown in Fig. 1, the ship-to-grid connection needs accurate measurements and considerations with an acceptable time for closing the circuit breakers.

There are certain requirements that must be met for successful paralleling of alternators like phase sequence of the three phases, voltage magnitude, frequency, and phase angle. After the synchronizing conditions are successfully checked, the switches will allow the ship to be connected to the grid. The process can be automated by using an automatic synchronizer system. When generator sets of a ship operate in parallel, the engine speed governor of each generator determines the proportional sharing of the total active power of the system. The electricity load sharing is achieved by decreasing or increasing fuel to the systems' engines. The control system of the generator sets controls and monitors the sharing of the total power load in proportion to the relative rating of the systems' generator sets.

III. DC-Link Connection Model

When AC power is converted to DC for connecting two AC networks with different frequency and voltage levels, the AC power is usually rectified and smoothed. Then, the power is routed to an inverter to obtain the final AC output. Because of the physical limitations on the design of the shipboard and terrestrial power systems, compact converter modules are most applicable for this problem. In addition, the developments in ac to dc to ac converters enable efficient digital control of active and reactive power flow. A DC-link connection is able to limit fault current through the use of power electronic converters. However, the challenge is that to transmit power via a DC-link,

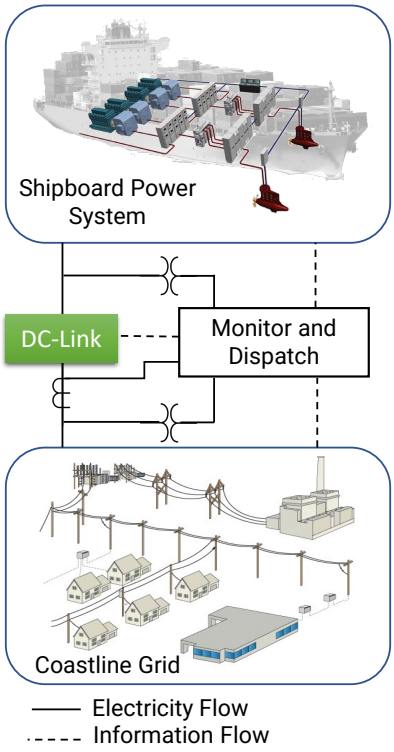

Fig. 1. Interconnection of the shipboard power system and coastline grid using a DC-link.

two converter stations are needed. The shipboard AC power needs be converted to DC, and then when it gets to the desired tie-in destination, the DC power should be converted back to AC power to be utilized in the grid.

A. AC to DC Converter

An AC to DC converter circuit relies on rectification. Based on back-to-back connected three-phase voltage-source converter units, converter systems have become one of the main building blocks for electronically-coupled DC units to the main utility grid. In this study, an AC to DC converter model with average values representation on digital simulation platforms is implemented in the modeling.

As illustrated in Fig. 2, the model is adjusted for a converter controlling for three-phase current injection I_{ref}^{abc} on the primary side, and employs the voltage source V_{ref} on the secondary side. In order to deal with low current harmonics at the AC side and controlling the DC voltage, pulse-width modulation (PWM) techniques are applied, which makes the rectification almost harmonic-free. In this case of the AC to DC converter model, a Phase-Locked Loop (PLL) is used to generate an output signal whose phase is related to the phase of an input voltage angle, θ. A basic PLL system consists of a phase detector, a loop filter, and a voltage-controlled oscillator. The phase difference between the input AC voltage phase and the estimated value would be detected by the phase detector. Then, the phase error is compensated by a low pass filter (such as a PI regulator) that is employed as a loop filter. At the end, the output of the loop filter is fed back to the voltage control unit as an integral unit, and the phase angle could be estimated. The estimated angle is used to convert the three-phase voltages V_{in}^{abc} and currents I_{in}^{abc} to DQ-frame quantities V_{in}^{dq} and I_{in}^{dq}, respectively. The resulted DQ-frame voltages are then used for estimating the phase of input voltages. As a result, the magnitudes of the voltage $|V_{in}^{dq}|$ and current $|I_{in}^{dq}|$ are computed, and used to replace the instantaneous primary-side voltage and current employed in the DC to AC converter model. Then, the output DC voltage of the converter could be adjusted based on load requirements. The primary-side current references, I_{ref}^{abc}, are calculated by multiplying the primary-side voltage magnitude and the measured secondary-side power. In order to be in phase with the primary-side voltages for the unity power factor, the generated θ is used. The secondary DC voltage source side, V_{ref}, is calculated based on the filtered primary-side voltage magnitude, $|V_{in}|$, with a turns ratio, n.

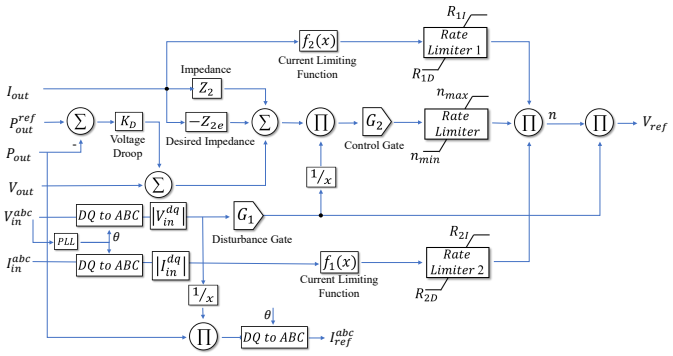

Fig. 2. The AC to DC converter model.

B. DC to AC Converter

A DC to AC converter is used to connect the AC output power of the DC-link to the shoreline grid. As shown in Fig. 3, to model the DC to AC converter, a current injection I_{ref} and a three-phase voltage source V_{ref}^{abc} are employed on the primary and secondary sides of the control block, respectively. The model is developed based on an ideal transformer with an adjustable turns ratio, n. The difference between the actual output power and the reference power would impact the reference secondary-side Root Mean Square (RMS) voltage, V_{out}^{abc} by droop control. The output of the previous stage is added to the converted AC current, I_{out}^{abc}, to compensate for the secondary-side voltage drop. The sum of the I_{out}^{abc} Z_2 and $k_D(P_{out}^{ref} - P_{out})$ and V_{out}^{abc}, with negative terms to include voltage drop for an emulated impedance of Z_{2e}, result in an effective voltage reference of V_e^*. The output and input quantities of the model are considered as per-unit values. After applying the filter of $G_1(s)$ on the primary-side voltage, the values of V_{in} and I are multiplied to reverse the voltage reference to obtain the reference turns ratio, n^*. To prevent the profligate of the disturbances on the primary voltage through the secondary side, the $G_1(s)$ filter represents a restriction

in the bandwidth of disturbances. To enforce limits on the maximum and minimum values of the turns ratio, a hard rate limiter is applied on the output of the control gate $G_2(s)$, which is designed to control the bandwidth of the converter outputs. The filtered primary-side voltage is multiplied by the actual turns ratio, n, to produce the secondary-side voltage reference, V_{ref}^{abc}. Two other branches are employed to represent the current limiting behavior of the converter.

$$Z_2(s) = R_1 - Z_2 + \frac{s(X_1 - Z_2)}{2\pi f b} \tag{1}$$

$$Z_{2e}(s) = R_1 - Z_{2e} \tag{2}$$

$$G_i(s) = \frac{1}{(\frac{s}{2\pi f c - G_i}) + 1} \tag{3}$$

where Z_2 is the base impedance on the secondary side. The $f(x)$ is a scale factor function for the primary-side current limit, with a value of 1 when $x \leq 1.2$ and 0 when $x \geq 1.35$. The current limiting functions $f_1(x)$ and $f_2(x)$ provide gains as the functions of the primary I_{in} and secondary I_{out}^{abc} currents, respectively. These gains are typically unity within the current limits of the converter, and tend to be zero as the current limits are approached. Rate limiters 1 and 2 allow these multiplicative factors to ramp down quickly, but ramp back to unity slowly, in order to avoid rapid oscillations when the current is limiting.

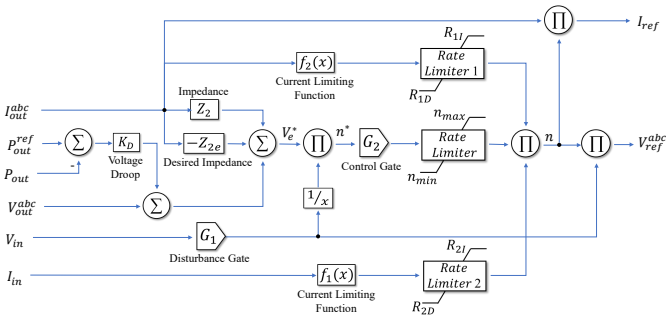

Fig. 3. The DC to AC converter model.

IV. Case Study and Numerical Results

It is assumed that the shipboard power system rating is 100 MW, including 3 main generators with a capability of 30 MW and one auxiliary generator with a capability of 10 MW. It is assumed that the propulsion motors and all other electrical loads like hotel, HVAC (heating, ventilation, and air conditioning) systems, and energy storage on the ship are OFF, when the ship connects to the grid to help restore the shoreline power. The 4-zone shipboard power system is modeled in the PSS@E. The dynamic models of the DC-Link converters are created by two different macros in PSS@NETOMAC, i.e., one for the ac to dc converter and the other for the dc to ac converter. In order to have one integrated dynamic model, the shipboard power system model is also imported into PSS@NETOMAC for dynamic simulations.

Different case studies have been performed to evaluate the efficiency and feasibility of ship-to-grid connection under various frequency and voltage levels in the shoreline grid. The simulations are initialized with power dynamic modeling, and then a contingency scenario is applied to the shoreline grid to analyze the transient behaviour of the interconnected systems. The ship-to-grid interconnection is modeled in PSS@NETOMAC, and the procedure is briefly described as follows:

- Step 1: Set up a PSS@NETOMAC project and prepare the parameters with standard models.
- Step 2: Prepare 3 partitions, i.e., shoreline grid, shipboard grid, and DC-link.
- Step 3: Define the power system topology and fixed frequency sources.
- Step 4: Couple the 3 partitions by power balances (sources and P/Q branches).
- Step 5: Specify signals to be analyzed.
- Step 6: Create a contingency event (i.e., 3-phase short-circuit) for the shoreline grid.
- Step 7: Perform simulations by "Calculate - Dynamics" and evaluate the results.

Time-domain transient behaviour of the control systems can be divided based on the timescale of the underlying dynamics [25], in the simulations of the electric grid ranging from less than a microsecond for wave phenomena up to minutes for thermodynamics simulations [26]. The dynamic simulations performed in this study are 0.5 second; the contingency event happens at 0.1 second after the start of the simulation, and the event lasts for 0.15 second. In this study, it is assumed that the simulations have a fixed time-step of 0.1 millisecond.

The main terrestrial grid is modelled as an AC source system without any in-service units. It is assumed that the main grid demands are totally supplied by the ship. The shipboard power system could only supply the AC terrestrial grid when the ship is in the synchronization mode to the main grid. As shown in Fig. 4(a), the contingency event in the terrestrial grid causes voltage drop in the terrestrial grid (represented by the red line). However, the voltage of the ship node after the DC-link remains in an acceptable voltage ratio (represented by the blue line). Thus, the shipboard grid voltage does not experience a lot of fluctuations during the contingency event occurred in the terrestrial grid.

In Fig. 4(b), the red line represents the power load of the terrestrial grid, shown as negative values. The power exported from the ship to the grid is represented by the blue line. During the contingency event at 0.1 s, the load of the system becomes zero because the protective relays separate the fault from the network. In the ship side, we observe some fluctuations but it is damped soon to become stable. When the ship is connected again to supply the grid at 0.25 s, it again presents stable behavior in both active and reactive power diagrams.

Another important fact that should be taken into account is the connection of two different networks with various system frequencies, which could be one of the most important advantages from the DC-link. Electrical ships are voyaging

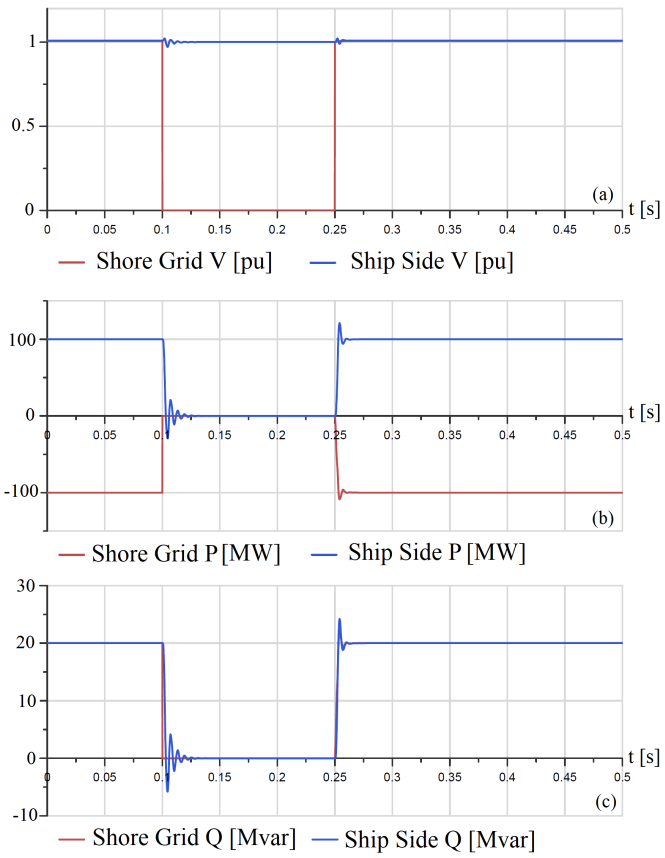

Fig. 4. Transient behavior of the (a) voltage, (b) active power, (c) reactive power, in both the terrestrial and shipboard networks.

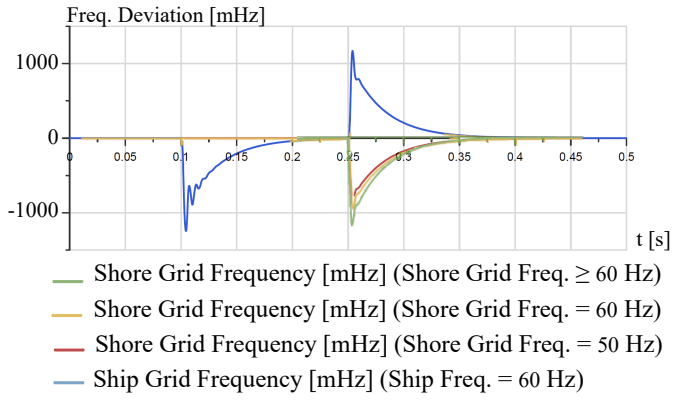

Fig. 5. Transient behavior of the frequency in both the terrestrial and shipboard power networks.

through different seas. Each shoreline grid might have its own operation characteristics like voltage level and frequency. To this end, it is assumed that the shipboard power system frequency is 60 Hz, while the shoreline grid frequency could be 50 Hz, 60 Hz, or higher. Figure 5 shows the transient behavior in both the terrestrial and shipboard grids after the contingency event, under different frequency settings. The blue line illustrates the ship frequency during the event. It is observed that when the frequency of the shoreline grid increases, the overshot of the frequency deviation from the nominal value would increase in the main grid side when the ship starts to supply power. However, the frequency deviation in the ship side does not experience specific changes. This is because that the DC-link separates both networks and does not allow any frequency deviation between different grids to enter into the shipboard power system.

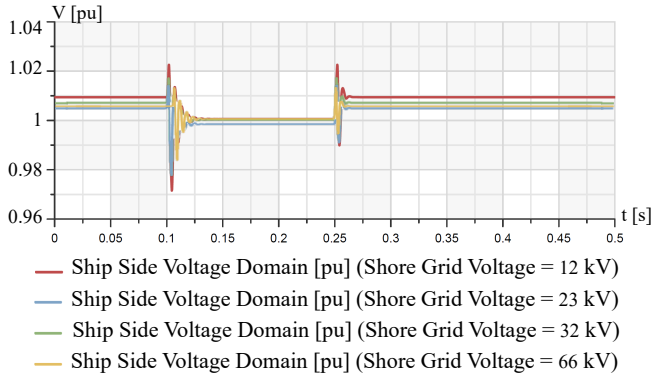

Fig. 6. Transient behavior of the voltage in the shipboard power system during the contingency event occurred in the main grid under various voltage levels.

The shipboard power system voltage is set at 6 kV. Similar to the various frequency ratios in Fig. 5, the simulation is repeated with different voltage levels. The different voltage levels of the shoreline power network lead to similar transient behavior of voltage in the ship side, as illustrated in Fig. 6. Overall, the DC-link is an effective solution for ship-to-grid to supply the main grid demands (even under different frequency levels) after disruptive events.

V. Conclusion

Extreme weather conditions inevitably lead to severe issues in power system infrastructures, resulting in power outages and customer quality deterioration, thereby increasing the risk of societal health and safety. This study evaluated the dynamic feasibility of ship-to-grid integration to enhance the reliability and resilience of both systems under extreme events, through integrated operation and control of both shipboard and shoreline power networks. By taking into account the unique designs in the electric ship equipment (such as the power conversion module, integrated power node center, propulsion motors, and energy storage module), a DC-link was proposed in this study for ship-to-grid connection with various voltage levels and system frequencies. The simulation results showed that the proposed DC-link was capable of preventing stability issues for the shipboard power system after contingencies occurred in the main grid, by minimizing the bus voltage and frequency deviation from the rated value.

Potential future research could consider an appropriate design of protection systems, to successfully assure proper protection to ship crews and equipment.

ACKNOWLEDGMENT

This material is based upon work sponsored by the Department of the Navy, Office of Naval Research under ONR award number N00014-20-1-2795. The United States Government has a royalty-free license throughout the world in all copyrightable material contained herein. Any opinions, findings, and conclusions or recommendations expressed in this material are those of the author(s) and do not necessarily reflect the views of the Office of Naval Research.

REFERENCES

[1] M. Yan, Y. He, M. Shahidehpour, X. Ai, Z. Li, and J. Wen, "Coordinated regional-district operation of integrated energy systems for resilience enhancement in natural disasters," *IEEE Transactions on Smart Grid*, vol. 10, no. 5, pp. 4881–4892, 2019.

[2] M. Ganjkhani, S. N. Fallah, S. Badakhshan, S. Shamshirband, and K.-w. Chau, "A novel detection algorithm to identify false data injection attacks on power system state estimation," *Energies*, vol. 12, no. 11, 2019.

[3] Z. Li, M. Shahidehpour, F. Aminifar, A. Alabdulwahab, and Y. Al-Turki, "Networked microgrids for enhancing the power system resilience," *Proceedings of the IEEE*, vol. 105, no. 7, pp. 1289–1310, 2017.

[4] A. B. SMITH, "2020 u.s. billion-dollar weather and climate disasters in historical context," Available at https://www.climate.gov/disasters2020 (2021/09/27.

[5] J. Xue, F. Mohammadi, X. Li, M. Sahraei-Ardakani, G. Ou, and Z. Pu, "Impact of transmission tower-line interaction to the bulk power system during hurricane," *Reliability Engineering System Safety*, vol. 203, p. 107079, 2020.

[6] H. Zhang, P. Wang, S. Yao, X. Liu, and T. Zhao, "Resilience assessment of interdependent energy systems under hurricanes," *IEEE Transactions on Power Systems*, vol. 35, no. 5, pp. 3682–3694, 2020.

[7] E. B. Watson and A. H. Etemadi, "Modeling electrical grid resilience under hurricane wind conditions with increased solar and wind power generation," *IEEE Transactions on Power Systems*, vol. 35, no. 2, pp. 929–937, 2020.

[8] L. Che and M. Shahidehpour, "Adaptive formation of microgrids with mobile emergency resources for critical service restoration in extreme conditions," *IEEE Transactions on Power Systems*, vol. 34, no. 1, pp. 742–753, 2019.

[9] S.-I. Park, S.-K. Kim, and J. K. Paik FREng, "Safety-zone layout design for a floating lng-fueled power plant in bunkering process," *Ocean Engineering*, vol. 196, p. 106774, 2020. [Online]. Available: https://www.sciencedirect.com/science/article/pii/S0029801819308753

[10] G. Sulligoi, A. Vicenzutti, and R. Menis, "All-electric ship design: From electrical propulsion to integrated electrical and electronic power systems," *IEEE Transactions on Transportation Electrification*, vol. 2, no. 4, pp. 507–521, 2016.

[11] A. Colavitto, A. Vicenzutti, D. Bosich, and G. Sulligoi, "Open challenges in future electric ship design: High-frequency disturbance propagation in integrated power and energy systems on ships," *IEEE Electrification Magazine*, vol. 7, no. 4, pp. 98–110, 2019.

[12] R. Xie, Y. Chen, Z. Wang, S. Mei, and F. Li, "Online periodic coordination of multiple pulsed loads on all-electric ships," *IEEE Transactions on Power Systems*, vol. 35, no. 4, pp. 2658–2669, 2020.

[13] M. Dabbaghjamanesh, S. Senemmar, and J. Zhang, "Resilient distribution networks considering mobile marine microgrids: A synergistic network approach," *IEEE Transactions on Industrial Informatics*, vol. 17, no. 8, pp. 5742–5750, 2021.

[14] S. Wen, T. Zhao, Y. Tang, Y. Xu, M. Zhu, S. Fang, and Z. Ding, "Coordinated optimal energy management and voyage scheduling for all-electric ships based on predicted shore-side electricity price," *IEEE Transactions on Industry Applications*, vol. 57, no. 1, pp. 139–148, 2021.

[15] A. Vicenzutti, F. Tosato, G. Sulligoi, G. Lipardi, and L. Piva, "High voltage ship-to-shore connection for electric power supply support in landing operations: An analysis," in *2015 IEEE Electric Ship Technologies Symposium (ESTS)*, 2015, pp. 364–369.

[16] P. Ghimire, M. Zadeh, E. Pedersen, and J. Thorstensen, "Dynamic efficiency modeling of a marine dc hybrid power system," in *2021 IEEE Applied Power Electronics Conference and Exposition (APEC)*, 2021, pp. 855–862.

[17] A. Maqsood, D. Oslebo, K. Corzine, L. Parsa, and Y. Ma, "Stft cluster analysis for dc pulsed load monitoring and fault detection on naval shipboard power systems," *IEEE Transactions on Transportation Electrification*, vol. 6, no. 2, pp. 821–831, 2020.

[18] R. A. Jacob, S. Senemmar, and J. Zhang, "Fault diagnostics in shipboard power systems using graph neural networks," in *2021 IEEE 13th International Symposium on Diagnostics for Electrical Machines, Power Electronics and Drives (SDEMPED)*, vol. 1, 2021, pp. 316–321.

[19] S. Senemmar and J. Zhang, "Deep learning-based fault detection, classification, and locating in shipboard power systems," in *2021 IEEE Electric Ship Technologies Symposium (ESTS)*, 2021, pp. 1–6.

[20] Y. Xu, H. Nian, and L. Chen, "Small-signal modeling and analysis of dc-link dynamics in type-iv wind turbine system," *IEEE Transactions on Industrial Electronics*, vol. 68, no. 2, pp. 1423–1433, 2021.

[21] M. Zolfaghari, G. B. Gharehpetian, and A. Anvari-Moghaddam, "Quasi-luenberger observer-based robust dc link control of uipc for flexible power exchange control in hybrid microgrids," *IEEE Systems Journal*, vol. 15, no. 2, pp. 2845–2854, 2021.

[22] A. Hota and V. Agarwal, "A novel three phase induction motor drive for ceiling fan application with improved dc-link utilization," in *2021 International Conference on Sustainable Energy and Future Electric Transportation (SEFET)*, 2021, pp. 1–5.

[23] P. Wang, Q. Wu, S. Huang, B. Zhou, and C. Li, "Distributed optimal voltage control strategy for ac grid with dc connection and offshore wind farms based on admm," *International Journal of Electrical Power Energy Systems*, p. 107802, 2021. [Online]. Available: https://www.sciencedirect.com/science/article/pii/S0142061521010206

[24] M. M. Biswas, T. Deese, J. Langston, H. Ravindra, K. Schoder, M. Steurer, H. Ginn, and C. Schegan, "Shipboard zonal load center modeling and characterization on real-time simulation platform," in *2021 IEEE Electric Ship Technologies Symposium (ESTS)*, 2021, pp. 1–9.

[25] S. Badakhshan, M. Ehsan, M. Shahidehpour, N. Hajibandeh, M. Shafie-Khah, and J. P. S. Catalão, "Security-constrained unit commitment with natural gas pipeline transient constraints," *IEEE Transactions on Smart Grid*, vol. 11, no. 1, pp. 118–128, 2020.

[26] D. Rimorov, J. Huang, C. F. Mugombozi, T. Roudier, and I. Kamwa, "Power coupling for transient stability and electromagnetic transient collaborative simulation of power grids," *IEEE Transactions on Power Systems*, vol. 36, no. 6, pp. 5175–5184, 2021.